JOURNAL of the MEXICAN CHEMICAL SOCIETY

https://www.jmcs.org.mx/

Article

Open Access

J. Mex. Chem. Soc. **2026**, *70(1):e2165*

Received November 6th, 2023
Accepted April 15th, 2024

http://dx.doi.org/10.29356/jmcs.v70i1.2165
e-location ID: 2165

Keywords:
Nanostructured lipid carriers, volatile oil, *Dipsacus asper*, storage stability

Palabras clave:
Portadores de lípidos nanoestructurados, aceite volátil, *Dipsacus asper*, estabilidad de almacenamiento

***Corresponding author:**
Xiaofeng Liang
email: XFLiang@swust.edu.cn
Phone: +8613547133875

ISSN-e 2594-0317

Nanostructured Lipid Carriers-Chitosan Carrier System for Loading of *Dipsacus Asper* Essential Oil: Preparation, Characterization, Antioxidant Study

Yu Zhang[1,2], Mengjiao Zhou[2], Jing Zou[1], Chaojun Li[1], Ming Kang[1], Xiaofeng Liang[1,2*]

[1]School of Materials and Chemistry, Southwest University of Science and Technology, Mianyang, 621010, China.
[2]Mianyang Key Laboratory of Traditional Chinese Medicine Resources Development and Utilization, Sichuan College of Traditional Chinese Medicine, Mian yang, 621010, China.

Abstract. *Dipsacus asper* essential oil (DEO) was encapsulated within a nanostructured lipid carrier (DEO-NLC), with chitosan (DEO-NLC-CS) subsequently applied as a surface coating. These carriers ' physicochemical and morphological properties, stability, in vitro release performance, and antioxidant activity were investigated. This study presents a new approach to address the challenges of Dipsacus essential oil's volatility and poor water solubility. The average diameter of DEO-NLC and DEO-NLC-CS were 68.90 ± 1.18 and 119.40 ± 1.40 nm, respectively, as determined by dynamic light scattering (DLS). Scanning electron microscope (SEM) and transmission electron microscope (TEM) confirmed both carriers were spherical-like coating structures, which confirmed the results of DLS. Attenuated total reflectance-Fourier transform infrared spectroscopy (ATR-FTIR) showed the successful physical capture of DEO in DEO-NLC and DEO-NLC-CS. The X-ray diffractogram of DEO-NLC and DEO-NLC-CS exhibited a wide high-intensity peak at 2θ = 15~25°, indicating that DEO was entrapped within NLC. It has been confirmed through differential scanning calorimetry (DSC) that the chitosan matrix successfully encapsulated DEO. In vitro release studies showed that both exhibited good sustained release properties. The antioxidant studies showed that blank NLC, DEO-NLC, and DEO-NLC-CS have good 1,1-diphenyl-2-picryl-hydrazyl radical (DPPH·) scavenging activities.

J. Mex. Chem. Soc. **2026**, *70(1):e2165*
Regular Issue

ISSN-e 2594-0317

Resumen. El aceite esencial de *Dipsacus asper* (DEO) se encapsuló dentro de un portador lipídico nanoestructurado (DEO-NLC), y posteriormente se aplicó quitosano (DEO-NLC-CS) como recubrimiento de superficie. Se investigaron las propiedades fisicoquímicas y morfológicas, la estabilidad, el rendimiento de liberación in vitro y la actividad antioxidante de estos portadores. Este estudio presenta un nuevo enfoque para abordar los desafíos de la volatilidad y la mala solubilidad en agua del aceite esencial de Dipsacus. El diámetro promedio de DEO-NLC y DEO-NLC-CS fue 68,90 ± 1,18 y 119,40 ± 1,40 nm, respectivamente, según lo determinado por dispersión dinámica de luz (DLS). El microscopio electrónico de barrido (SEM) y el microscopio electrónico de transmisión (TEM) confirmaron que ambos portadores eran estructuras de recubrimiento esféricas, lo que confirmó los resultados de la DLS. La espectroscopia infrarroja de transformada de Fourier de reflectancia total atenuada (ATR-FTIR) mostró la captura física exitosa de DEO en DEO-NLC y DEO-NLC-CS. El difractograma de rayos X de DEO-NLC y DEO-NLC-CS mostró un pico amplio de alta intensidad en $2\theta = 15\sim25°$, lo que indica que el DEO quedó atrapado dentro de NLC. Se ha confirmado mediante calorimetría diferencial de barrido (DSC) que la matriz de quitosano encapsuló con éxito el DEO. Los estudios de liberación in vitro demostraron que ambos presentaban buenas propiedades de liberación sostenida. Los estudios de antioxidantes mostraron que los blancos NLC, DEO-NLC y DEO-NLC-CS tienen buenas actividades de eliminación del radical 1,1-difenil-2-picril-hidrazilo (DPPH·).

Introduction

With the rapid increase in the global population and the use of antibiotics, multidrug-resistant strains (MDR) and extremely drug-resistant strains (XDR) have become a huge threat to secondary infections [1]. Currently, the treatment of secondary infection after recovery is still based on long-term antibiotic treatment. The intensive and improper use of antibiotics and insufficient course of antibiotic treatment not only accelerate the emergence of multidrug-resistant strains and extremely drug-resistant strains but also aggravate the pain of patients [2-4]. Currently, there is a shortage of antibiotics available for clinical use. Researchers have suggested that combining existing antibiotics with natural compounds, such as plant essential oils, may be an effective solution to address this issue; combining EOs/volatile compounds and antibiotics can exert a multi-target antimicrobial activity, effectively reducing or reversing microbial resistance [5-7].

EOs are hydrophobic substances obtained mainly by steam distillation or extraction from plant tissues like leaves, roots, flowers, and fruits [8]. Most herbs are rich in bioactive substances like EOs and have a wide range of biological and antibacterial activities due to their complex components [9]. Furthermore, the low potential for microbial resistance development associated with EOs stems from their multi-componential nature, enabling multi-target activity against multidrug-resistant (MDR) bacteria. This attribute represents a significant advantage over the single-target effects of conventional antibiotics [10-13].

Dipsacus asper (*Dipsacus asper* wall. Ex Henry) is a medicinal plant in China. As stated, it is a member of the family Caprifoliaceae and the Lamiaceae, and the main medicinal part is its root. The plant is widely distributed in China's southwest and central regions [14-16]. The above plant has a complex composition and various pharmacological effects, including anti-osteoporosis, bone protection, uterine protection, antibacterial, etc [17]. As one of the main components of *Dipsacus asper*, the essential oil of *Dipsacus* asper (DEO) shows good pharmacological effects in anti-tumor, antibacterial, and other aspects, which is expected to become an alternative drug for combined antibiotic therapy [18]. However, DEO is characterized by active and volatile chemical properties, rendering it susceptible to external influences. Owing to its reactivity, it is prone to oxidation and decomposition. Furthermore, its limited solubility in water constrains its application and impedes further development [19].

Encapsulation technology can protect DEO from adverse environmental conditions, which is an effective method to protect DEO from environmental impact and prolong the inhibition of microorganisms [20]. Nanostructured lipid carriers (NLC) can serve as a promising carrier system to improve the bioavailability of lipophilic substances, with simpler preparation methods and higher encapsulation rates than liposomes and nano-emulsions. They can be used as a perfect substitute for both [21,22]. However, NLC still has relatively poor storage stability [23].

Coating polymers on the surface of NLC can improve its storage stability [24,25]. Natural polymers are widely used in various fields due to their reliable mechanical and material properties. Among them, chitosan

J. Mex. Chem. Soc. **2026**, *70(1):e2165*
Regular Issue

ISSN-e 2594-0317

is a linear cationic polysaccharide with a high degree of biodegradability, antibacterial, non-toxic, and good biocompatibility. It is used in biomedical applications widely. Its coating on the surface of NLC can avoid NLC aggregation and fusion [26], prevent drug leakage [27], improve drug retention rate, effectively reduce the degree of lipid oxidation [28], and enhance the thermal stability of NLC [29].

The main purpose of this study is to obtain DEO-loaded NLC (DEO-NLC) and DEO-loaded NLC of chitosan (DEO-NLC-CS) by a simple and efficient melt emulsification-ultrasonic method, to prolong the storage time of DEO and improve its bioavailability, which provides a way for subsequent antibiotics combined with natural compounds. The physicochemical properties of the prepared blank NLC, DEO-NLC, and DEO-NLC-CS were studied, including average particle size, Zeta potential, encapsulation efficiency, drug loading, thermal analysis, wide-angle X-ray diffraction, in vitro release study and antioxidant activity.

Materials and methods

Materials

Dipsacus asper was purchased from Zhenyaotang Pharmaceutical Co., Ltd. (Jiangxi, China); Glycerol Monostearate (GM), Glyceryl Octanoate (GO), Tween 80 (CP), Chitosan (degree of deacetylation 80 %, MW = 500000) and Soybean Lecithin (SL) were provided by Shanghai Macklin Biochemical Co., Ltd. (Shanghai, China); 1,1-diphenyl-2-picryl-hydrazyl radical (DPPH·) was provided by Sinopharm Chemical Reagent Co., Ltd. (Shanghai, China); All other chemicals were of analytical grade.

Extraction of *Dipsacus asper* essential oil

Dipsacus asper is a genuine medicinal material in China, and its main medicinal component is its root [30]. In this experiment, a supercritical CO_2 extraction device was used. The *D. asper* powder was extracted using ethanol as the carrier agent (all samples were crushed and passed through 20 mesh sieve) [31-33]. After extraction, the unstable target product was removed using a rotary evaporator to extract the liquid. The essential oil was obtained by vacuum pumping for 10 minutes. Keep it in the refrigerator at 4 ℃.

Gas chromatography (GC)–Mass spectrometer analysis (MS)

Gas chromatography condition: Nonpolar SH - Rxi - 5 Sil MS capillary column (30 m × 0.25 mm ×0.25 μm) was used, with helium as the carrier gas. The injection temperature was 290 ℃, and the column box temperature was controlled using a programmed heating scheme. The initial temperature of the column was set at 50 ℃, which was held for 5 min, then it was increased to 200 ℃ at 10 ℃/min for 2 min and finally increased to 290 ℃ at 5 ℃/min for 10 min. The injection volume was 1μL, with a shunt ratio 10:1. The column flow was maintained at 1.0 mL/min, and the solvent delay time was set at 3 min.

Conditions for mass spectrometry: Ion source ~ electron bombardment ion source (EI); source temperature ~ 200℃; interface temperature ~ 220℃; detection voltage ~ 0.8 kV; mass scanning range (m/z) ~ 33 to 700 amu; electronic energy ~ 70 eV [34].

Preparation of DEO-loaded NLC and DEO-loaded NLC of chitosan

The preparation steps of DEO-NLC and DEO-NLC-CS are shown in Fig. 1 was prepared by melt emulsification ultrasonic method, as previously described by Wang et al., with slight modifications [35,36]. In brief, a mixture comprising 0.05 g of caprylic capric triglyceride (CAT), 0.05 g of glyceryl monostearate (GM), and 0.1 g of DEO was melted at 73 °C to form the oil phase. Simultaneously, a solution containing 0.4 g of soy lecithin and 0.4 g of Tween 80 dissolved in 20 mL of ultrapure water was prepared and melted at 73 °C to constitute the aqueous phase. Subsequently, the aqueous phase was slowly added to the oil phase under continuous stirring at 600 rpm and at a constant temperature. Stirring was maintained for 20 min until colostrum formation occurred. Colostrum was obtained by ultrasound (ultrasonic amplitude 80 %, open for 5 s, stop for 5 s) for 15 min, cooled and solidified in an ice water bath for 5 min, and then passed through 0.22 μm microporous membrane. The preparation method of DEO-NLC-CS was almost unchanged according to the method of Lee et al. [37]. One hundred mL of 1 % (V/V) glacial acetic acid solution was prepared. To this, 10 mL of 1 % (V/V) glacial acetic acid was added to 0.01 g chitosan powder and stirred until a colorless viscous liquid was formed. 10 mL of the

J. Mex. Chem. Soc. **2026**, *70(1):e2165*
Regular Issue

ISSN-e 2594-0317

above solution was mixed with 10 mL of hot DEO-NLC and stirred at 60 °C for 2 h. The mixture was ultrasonically dispersed and cooled at room temperature to obtain the product.2.5 Physicochemical characterization.

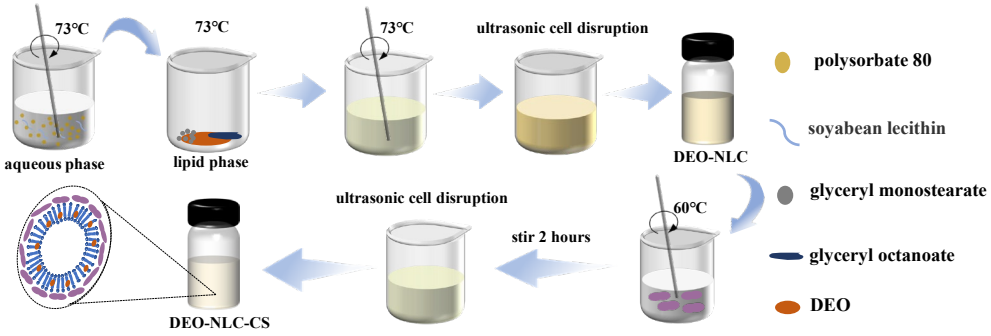

Fig. 1. Flow chart of DEO-NLC and DEO-NLC-CS preparation.

Particle diameter and Zeta potential

After 24 h of preparation, the average diameter, polydispersity index (PDI), and Zeta potential of DEO-NLC and DEO-NLC-CS were determined by 90 plus laser particle size analyzer and Zeta potential analyzer (Malvern Instruments, UK) at 25 °C. Before the test, the dispersions were diluted 10-fold with deionized water to prevent multi-scattering due to the interparticle interaction of measurements made in triplicate. The Zeta diameters were utilized to calculate their zeta potential value automatically.

Morphological characterization

The transmission electron microscope (TEM) was used to observe whether the prepared object had a coating structure. Before the analysis began, a wax plate was taken, and a copper mesh containing the supporting film was placed on it. Then, 5 µL of DEO-NLC and DEO-NLC-CS were added dropwise on the membrane and left to dry naturally. After that, 5 µL of 2 % phosphotungstic acid was added dropwise, excess liquid was absorbed with filter paper, and the samples were observed under the TEM. The shape and surface analysis of the DEO-NLC and DEO-NLC-CS formulations were observed by scanning electron microscopy (SEM). Before the analysis, the DEO-NLC and DEO-NLC-CS nanosuspensions were placed on a double-side carbon tape mounted onto an aluminum stud and dried in a desiccator. After these procedures, the freeze-dried nanoparticles were placed on the conductive adhesive and observed by SEM.

Fourier-transform infrared (ATR-FTIR) spectroscopy

The interactions between DEO, DEO-NLC, and chitosan were studied using ATR-FTIR. All samples were freeze-dried before scanning. ATR-FTIR spectra of DEO, NLC, DEO-NLC, and DEO-NLC-CS beads in the 4000 to 500 cm^{-1} range were recorded more than 32 times.

Measurement of nanoparticles crystallinity by X-ray diffraction (XRD) analysis

XRD is a useful technique for evaluating lipid arrangement and phase behavior and characterizing lipid structure. The presence of liquid lipids does not affect solid lipid polymorphisms [38-40]. Before the scan, all samples were freeze-dried. Then, measurements are taken using the PertPro diffractometer, which controls its accelerating voltage of 40 kV and filament current of 40 mA with Cu Kα radiation and graphite monochromator, the dried NLC, DEO-NLC, and DEO-NLC-CS hydrogel beads were measured from 10° to 80°, using a step size of 0.03° at an angular speed of 2 °/min.

Thermal analysis

After drying, the sample is precisely weighed and placed in an aluminum pan with a lid. During the scanning process, heating is performed at a heating rate of 5 °C/min over a temperature range of 0 to 200 °C and nitrogen purging at a flow rate of 20 mL/min.

http://dx.doi.org/10.29356/jmcs.v70i1.2165

J. Mex. Chem. Soc. **2026**, *70(1):e2165*
Regular Issue

ISSN-e 2594-0317

Determination of loading parameters

The encapsulation efficiency (EE%) and loading capacity (LC%) of the DEO-NLC and DEO-NLC-CS by Fatemeh et al. [40],with almost no modification. Centrifugation was used to separate free and encapsulated DEO. Briefly, 1 mL of DEO-NLC and 7 mL of 50 % (w/w) ethanol were added to the ultrafiltration tube. Then, the above mixed solution was centrifuged at 4000 rpm for 5 min. The bottom filtrate was collected and diluted with 50% (w/w) ethanol, and its absorbance of the free DEO was measured by an ultraviolet-visible spectrophotometer at λ_{max} = 272 nm. Retain the solution at the upper end of the ultrafiltration tube, add 1 ml of chloroform, and shock for 5 minutes. The absorbance of the encapsulated DEO was tested at λ_{max} = 272 nm. Three times in parallel. In the mass concentration range of 0.1 ~ 2 mg/mL, the amount of DEO was calculated by the standard curve: $y = 0.5727\,x + 0.0848$, and the correlation coefficient R^2 = 0.9979 (n=6). Embedding parameters are determined as equations:

$$EE_1\% = \frac{Amount\ of\ the\ encapsulated\ DEO}{(Amount\ of\ the\ encapsulated\ DEO + Amount\ of\ the\ free\ DEO)} \times 100\% \quad (1)$$

$$EE_2\% = 1 - \frac{Amount\ of\ the\ free\ DEO - Chitosan\ sol}{Amount\ of\ initial\ DEO} \times 100\% \quad (2)$$

$$LC\% = \frac{Amount\ of\ encapsulated\ DEO}{(Amount\ of\ total\ lipids - total\ of\ DEO)} \times 100\% \quad (3)$$

***In-vitro* release study**

The *in-vitro* release studies of pure DEO DEO-NLC and DEO-NLC-CS were studied by dialysis [23]. In general, DEO is a hydrophobic substance. The solubility of DEO in the receptor medium can be increased by adding ethanol, according to the mandatory requirement of the release study, a 7:3 (V/V) mixture of phosphate-buffered saline (PBS) and an ethanol solution at pH = 7.4 as the acceptor phase to provide reasonable absorption condition. Before the study, 2 mL of pure DEO, DEO-NLC, and 2 mL DEO-NLC-CS to the dialysis bag, respectively. They were immersed in a 50 mL receptor phase and stirred at a rotor speed of 150 r/min for 48 h at 37 °C. At the selected time point, 2 mL of each sample was replaced with an equal volume of fresh receptor phase to maintain a constant volume. Finally, the sample was determined at 272 nm.

Storage stability study

During the storage of the sample, oxidation, and heating can lead to the degradation of DEO. DEO-NLC and DEO-NLC-CS were stored at 25 °C for one month, the average particle size, Zeta potential, and PDI of the above two particles were detected on the first day, the seventh day, the fourteenth day, the twenty-first day, and the twenty-eighth day to explore their storage stability at 25 °C.

Determination of the 1,1-diphenyl-2-picryl-hydraxyl radical (DPPH·) scavenging capacity

DPPH has been widely used to evaluate the antioxidant activity of various chemicals. The DPPH scavenging ability of DEO-NLC and DEO-NLC-CS were measured to characterize their antioxidant activity. These methods were based on the method described by Hu et al., with slight modifications [41]. Firstly, 4 mg of DPPH powder was added to ethanol to prepare a DPPH solution of 0.08 mg/mL. The DEO-NLC and DEO-NLC-CS dispersion were dissolved in ultrapure water to prepare sample solutions with 50, 100, 200, 400, and 600 mg/mL mass concentrations, respectively. Then, the mixture of 2.0 mL DPPH solution and 2 mL anhydrous ethanol was prepared as the control (A_0), the mixture of 2.0 mL DPPH solution and 2.0 mL sample solution with different concentrations (A_1) and the mixture of 2.0 mL anhydrous ethanol and 2.0 mL essential oil sample solution (A_2) were prepared. The above three solutions were mixed and placed in the dark for 30 min. The absorbance was measured at 517 nm by ultraviolet spectrophotometer. The inhibition rate formula is as follows:

$$DPPH\ scavenging\ ability = \frac{(A_0 + A_2 + A_1)}{A_0} \times 100\% \quad (4)$$

http://dx.doi.org/10.29356/jmcs.v70i1.2165

J. Mex. Chem. Soc. **2026**, *70(1):e2165*
Regular Issue

ISSN-e 2594-0317

Statistical analysis

All experiments were performed as mean ± standard deviation, n = 3. The Kruskal - Wallis test was used for comparisons. All tests were analyzed using SPSS 26.0; $P < 0.05$ was statistically significant.

Results and discussion

GC-MS analysis

GC-MS analyzed the main components of the essential oil in D. asper, and the relative content of each component was calculated using the peak area normalization method. It can be seen from Table 1 that a total of 46 compounds were detected in the essential oil of *D. asper*. Among them, the compounds with relative percentage content greater than 2 % were hexadecanoic acid (8.93 %), hexadecanoic acid, ethyl ester (4.22 %), linoleic acid ethyl ester (3.91 %), ethyl alpha -linolenate (3.13 %), capryl palmitate (2.54 %), clionasterol (10.51 %). The relative content of linoleic acid (1.90 %), ethyl n-octadecanoate (1.05 %), clionasterol (1.82 %), campesterin (1.90 %), and lanoster (1.04 %) were more than 1 %.

Table 1. Chemical components of DEO.

R.T/ min	Compounds	Molecular Formula	Relative content/ %	Similarity / %
4.04	Acetic acid n-propyl ester	$C_5H_{10}O_2$	0.28	86
4.215	Acetal	$C_6H_{14}O_2$	0.73	95
7.602	Butyrolactone	$C_4H_6O_2$	0.25	95
10.991	Linalol	$C_{10}H_{18}O$	0.68	96
11.065	Nonaldehyde	$C_9H_{18}O$	0.05	92
13.11	1-Thia-3-azaindene	C_7H_5NS	0.17	85
14.177	2-methyInaphthalene	$C_{11}H_{10}$	0.29	92
14.407	1-Methylnaphthalene	$C_{11}H_{10}$	0.12	94
19.19	2-Methylhexacosane	$C_{27}H_{56}$	0.26	90
21.013	Neophytadiene	$C_{20}H_{38}$	0.20	93
21.388	Phthalic acid	$C_{26}H_{42}O_4$	0.12	85
22.384	Hexadecanoic acid, methyl ester	$C_{17}H_{34}O_2$	0.31	88
22.947	Hexadecanoic acid	$C_{16}H_{32}O_2$	8.93	97
23.457	Hexadecanoic acid, ethyl ester	$C_{18}H_{36}O_2$	4.22	95
25.037	9,12-Octadecadienoic acid, ethyl ester	$C_{20}H_{36}O_2$	0.18	86
25.64	cis,cis-Linoleic acid	$C_{18}H_{32}O_2$	1.90	94
26.068	Linoleic acid ethyl ester	$C_{20}H_{36}O_2$	3.91	96

J. Mex. Chem. Soc. **2026**, *70(1):e2165*
Regular Issue

ISSN-e 2594-0317

R.T/ min	Compounds	Molecular Formula	Relative content/ %	Similarity / %
26.162	Ethyl alpha -linolenate	$C_{20}H_{34}O_2$	3.13	89
26.261	Ethyl (9Z)-9-octadecenoate	$C_{20}H_{38}O_2$	0.36	92
26.569	Ethyl n-octadecanoate	$C_{20}H_{40}O_2$	1.05	95
27.855	1-Methylpyrene	$C_{17}H_{12}$	0.18	90
28.173	Hexatriacontane	$C_{36}H_{74}$	0.17	94
28.439	2-Ethylhexyl trans-4-methoxycinnamate	$C_{18}H_{26}O_3$	0.09	93
28.439	Octinoxate	$C_{18}H_{26}O_3$	0.09	93
29.481	Ethyl arachidate	$C_{22}H_{44}O_2$	0.31	91
29.592	Tetracontane	$C_{40}H_{82}$	0.16	91
29.592	Triacontane	$C_{30}H_{62}$	0.16	90
30.924	Capryl palmitate	$C_{24}H_{48}O_2$	2.54	94
31.275	Phthalic acid, di(oct-3-yl) ester	$C_{24}H_{38}O_4$	0.20	91
31.338	Bis(2-ethylhexyl) phthalate	$C_{24}H_{38}O_4$	0.49	93
32.163	Ethyl docosanoate	$C_{24}H_{48}O_2$	0.15	90
33.507	Tetracosane	$C_{24}H_{50}$	0.23	92
33.507	Dotriacontane	$C_{32}H_{66}$	0.23	91
33.507	Tetratriacontane	$C_{34}H_{70}$	0.23	90
33.507	2-Methyloctacosane	$C_{29}H_{60}$	0.23	90
34.708	Tetrapentacontane	$C_{54}H_{110}$	0.11	89
34.708	Tetracontane	$C_{40}H_{82}$	0.11	88
34.864	Squalene	$C_{30}H_{50}$	0.66	93
35.868	Hexacontane	$C_{60}H_{122}$	0.37	93
36.175	(R)-2,7,8-Trimethyl-2-((3E,7E)-4,8,12-trimethyltrideca-3,7,11-trien-1-yl) chroman-6-ol	$C_{28}H_{42}O_2$	0.45	89
38.432	Tetrapentacontane	$C_{54}H_{110}$	0.54	91
39.065	Clionasterol	$C_{29}H_{50}O$	1.82	91
39.435	(24Z)-Stigmasta-5,24(28)-dien-3-ol	$C_{29}H_{48}O$	0.40	91
40.577	Campesterin	$C_{28}H_{48}O$	1.90	90

http://dx.doi.org/10.29356/jmcs.v70i1.2165

J. Mex. Chem. Soc. **2026**, *70(1):e2165*
Regular Issue

ISSN-e 2594-0317

42.286	Clionasterol	$C_{29}H_{50}O$	10.51	90
44.302	Lanster	$C_{30}H_{50}O$	1.04	89

Physicochemical characterization

Particle diameter, PDI, and Zeta potential

The average diameter and PDI of the DEO-NLC dispersion were 68.90 ± 1.18 nm and 0.252 ± 0.013, respectively (Fig. 2**(a)**). The average diameter and PDI of the DEO-NLC-CS were 119.40 ± 1.40 nm and 0.253 ± 0.003, respectively (Fig. 2**(e)**). All the above diameter distributions were less than 0.5. The particle diameter increased after DEO-NLC was coated with chitosan, and the electrostatic interaction of chitosan with DEO-NLC was confirmed.

It is generally believed that the system with a Zeta potential of -30 ~ -60 mV is stable [42]. Although the Zeta potential of DEO-NLC was -27.8 ± 1.20 mV, the prepared particles were clear and transparent, and no aggregation occurred. The Zeta potential of DEO-NLC-CS was 30.71 ± 2.34 mV. The Zeta potential of the DEO-NLC-CS that was prepared became positively charged due to the presence of chitosan, which carries an amino group with a positive charge. On the other hand, the principal component of NLC is a phospholipid, which has a negative charge. The two particles were combined through electrostatic interaction, and the potential was represented by the outermost layer of chitosan [23,43].

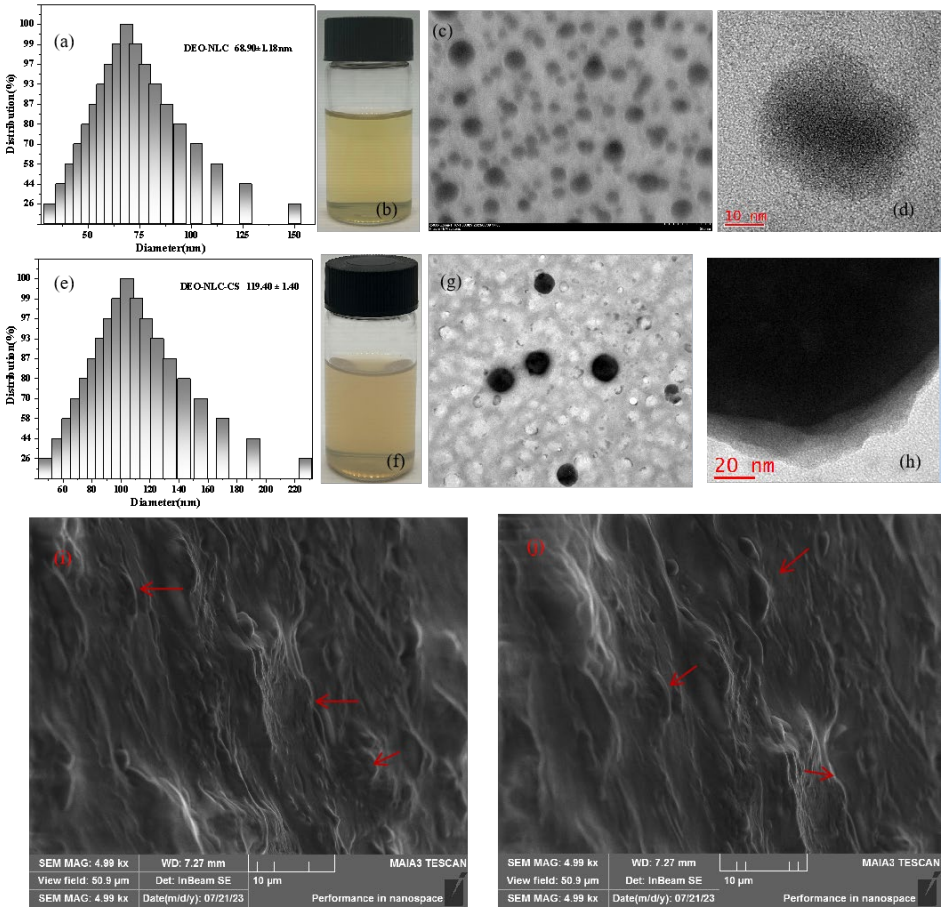

Fig. 2. (a), **(b)**, **(c)**, **(d)**, and **(i)** are the DLS histogram, visual image, TEM image, TEM local amplification image and SEM image of DEO-NLC after freeze-drying, respectively; **(e)**, **(f)**, **(g)**, **(h)**, and **(j)** are the DLS histogram, visual image, TEM image, TEM local magnification image and SEM image of DEO-NLC-CS, respectively.

http://dx.doi.org/10.29356/jmcs.v70i1.2165

J. Mex. Chem. Soc. **2026**, *70(1):e2165*
Regular Issue

ISSN-e 2594-0317

Table 2. Particle diameter, polydispersity index, Zeta potential value of DEO-NLC and DEO-NLC-CS (mean ± SD, n=3).

The type of particle	Particle diameter (nm)	Zeta potential (mV)	Polydispersity (PDI)
DEO-NLC	68.90 ± 1.18	-27.80 ± 1.20	0.252 ± 0.013
DEO-NLC-CS	119.40 ± 1.40	30.71 ± 2.34	0.324 ± 0.003

Morphological characterization

From the perspective of the macroscopic morphology, when viewed under natural light, the DEO-NLC appears clear and transparent with a pale yellow opalescent (Fig. 2**(b)**). After slight shaking, the level was uniform, the distribution was even, and there were no visible particles at the bottom. Similarly, DEO-NLC-CS produces a similar effect; DEO-NLC-CS also observed a similar phenomenon (Fig. 2**(f)**).

From the perspective of microscopic morphology, the prepared DEO-NLC and DEO-NLC-CS were spherical-like particles (Fig. 2**(c)**, 2**(g)**), with no adhesion between particles, small particle diameter difference, and uniform distribution; the above particles all had obvious coating structure (Fig. 2**(d)**, 2**(h)**), there is no adhesion between the particles, indicating that the material is successfully prepared. It can be seen that DEO-NLC and DEO-NLC-CS are spherical particles with uniform distribution (Fig. 2**(i)**, 2**(j)**).

Fourier-transform infrared (FTIR) spectroscopy

The IR spectra for the pure DEO, DEO-NLC, and DEO-NLC-CS are presented in Fig. 3**(a)**. Chitosan powder (CS) contained characteristic peaks in 1159 cm^{-1} (Amine) 2900 cm^{-1} (C-H stretching) [3420 cm^{-1} (O-H stretching)] 1645 cm^{-1} (C=O stretching) 1603 cm^{-1} (NH_2 bending) and 1662 cm^{-1} (amide I) [23]. As shown in Fig. 3**(a)**, the IR spectrum of pure DEO showed a series of characteristic absorption peaks in 3353 cm^{-1} (O-H) 2850~2960 cm^{-1} (Aliphatic CH_3 and CH_2) 1454 cm^{-1} [$(CH_2)n$] 1380.95 cm^{-1} [$(-CH(CH_3)_2)$]. The blank NLC was made of auxiliary materials other than DEO. The main functional groups in the spectra of the blank NLC, DEO-NLC, and DEO-NLC-CS vibrate almost identically. Still, the characteristic peaks of the pure DEO migrate or disappear. The results showed that there was a physical interaction between the blank NLC, DEO-NLC, and DEO-NLC-CS, and there was no chemical interaction and no intermolecular interaction [44], indicating that DEO was successfully coated in DEO-NLC and DEO-NLC-CS.

Measurement of nanoparticles crystallinity by X-ray diffraction (XRD)analysis

Glyceryl monostearate (GM) has a highly ordered β or β' crystal structure that leaves less space for active substances, causing drug leakage. [45,46]. As shown in Fig. 3**(b)**, there was no strong characteristic diffraction peak of GM in the blank NLC, it only had a weak diffraction peak, indicating that the crystal form of GM changed, and the blank NLC was successfully prepared. After the addition of DEO, the crystallinity decreased because DEO was not only a bioactive substance but also a special liquid lipid, resulting in more cavities and providing greater space and higher solubility for itself. After coating with chitosan, the crystallinity changed again. The above changes may be because chitosan is a crystal, which has no chemical interaction with DEO-NLC. Only physical coating is carried out, verifying the results in ATR-FTIR [47].

Thermal analysis

The release of the bioactive may be triggered by the melting of the lipid matrix, therefore it is important to access the thermal behavior of the nanostructured lipid carriers [48]. Differential scanning calorimetry (DSC) is widely used to evaluate drug melting behavior and polymorphisms in NLC [49]. As shown in Fig. 3**(c)**, the blank NLC showed a broad thermal spectrum, indicating that the particle was in a partially crystalline mixture or polycrystalline state of compounds with different melting points. With the addition of DEO, the thermal spectrum of NLC shifts to a lower melting peak, and the interaction between lipids and bioactive substances occurs, consistent with Miranda et al.'s view [21]. Similarly, the melting peak of DEO-NLC-CS broadens at about 130 °C and moves to a lower temperature. The decrease in melting point may be related to chitosan encapsulation [33].

J. Mex. Chem. Soc. **2026**, *70(1):e2165*
Regular Issue

ISSN-e 2594-0317

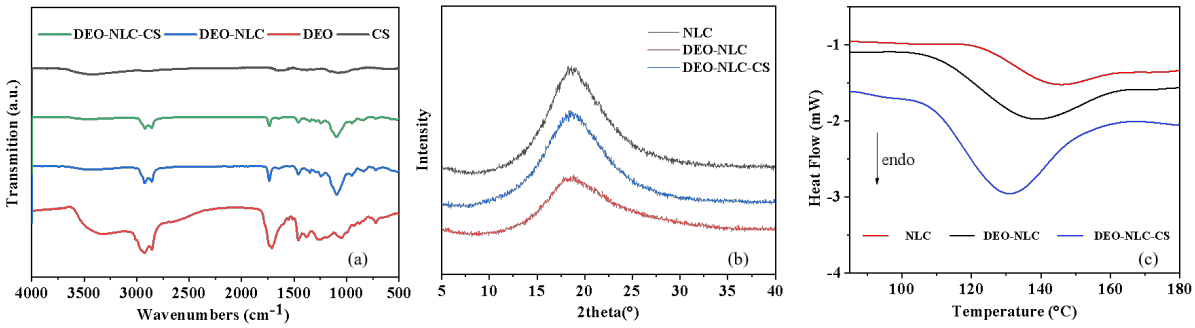

Fig. 3. (a) ATR-FTIR spectra; **(b)** XRD diffractograms; **(c)** DSC melting curves.

Determination of encapsulation efficiency (EE%) and loading capacity (LC%)

The EE% and LC% are crucial parameters for assessing the quality of lipid nanoparticle formulations [21]. The EE% of the DEO-NLC was over 80 %, indicating that the prepared DEO-NLC had an excellent coating rate (Fig. 4**(a)**). The high EE% of DEO-NLC due to its lipophilicity, and the distribution in the lipid matrix of NLC is higher than in the aqueous phase. The EE% of DEO-NLC-CS (90.76 ± 0.34 %) was significantly ($P < 0.05$) higher than DEO-NLC (83.14 ± 1.43 %), which may be due to the increase of particle size after chitosan coating DEO-NLC, creating more space for the encapsulation of bioactive substances, resulting in higher EE% (Fig. 4**(a)**).

In addition, The LC% of DEO-NLC was 17.39 ± 0.10 %, and the DEO-NLC-CS was 18.82 ± 0.23 % (Fig. 4**(b)**). The LC% of DEO-NLC-CS was higher than that of DEO-NLC. The electrostatic interaction between chitosan and DEO-NLC may have further ensured the high LC% of DEO-NLC-CS [20].

The above results indicate the prepared DEO-NLC and DEO-NLC-CS achieved the ideal encapsulation efficiency in this study.

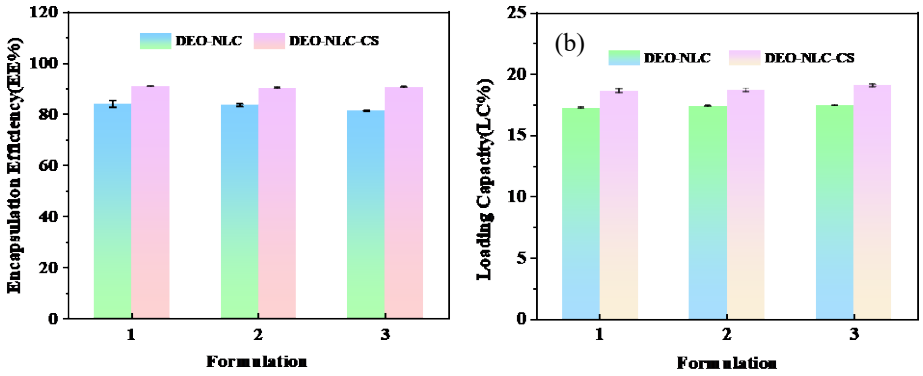

Fig. 4. (a) The entrapment efficiency (EE%); **(b)** loading capacity (LC%).

Table 3. EE% and LC%.

Number	EE （%）	LC （%）
DEO-NLC	84.21 ± 1.29	17.26 ± 0.06
DEO-NLC	83.70 ± 0.58	17.42 ± 0.03

http://dx.doi.org/10.29356/jmcs.v70i1.2165

J. Mex. Chem. Soc. **2026**, *70(1):e2165*
Regular Issue

ISSN-e 2594-0317

Number	EE（%）	LC（%）
DEO-NLC	81.52 ± 0.13	17.47 ± 0.02
DEO-NLC-CS	91.09 ± 0.11	18.66 ± 0.16
DEO-NLC-CS	90.41 ± 0.22	18.71 ± 0.14
DEO-NLC-CS	90.80 ± 0.17	19.09 ± 0.11

In-vitro release study

The standard curve equation of the solution drawn with phosphate buffer solution as the solvent is shown in Fig. 5**(a)**. Therefore, in the concentration range of 0.1~2.0 mg/mL, the equation was used for the *in vitro* release study.

Within 0.5~1h of dialysis, the pure DEO had a sudden release phenomenon, and the released mass reached 0.75 mg (Fig. 5**(b)**). Compared with the burst release behavior of pure DEO,DEO-NLC and DEO-NLC-CS showed better-sustained release performance. After 1 h of release, DEO-NLC and DEO-NLC-CS only released about 0.275 mg and 0.159 mg of DEO, respectively. The release of DEO in DEO-NLC is activated by the hydrophobic interaction between Tween 80 contained in the particle itself and other lipids or the melting of the hydrophobic core at 37 °C, leading to the dissociation of the nanostructure [41,50]. In contrast, DEO-NLC-CS had a more stable nanostructure due to the positive charge of the outer chitosan and the electrostatic interaction of the inner negatively charged nanostructured liposomes. DEO-NLC was completely released at 24 h, while DEO-NLC-CS was completely released at 48 h. It confirmed the prepared DEO-NLC-CS had better sustained release performance than DEO-NLC.

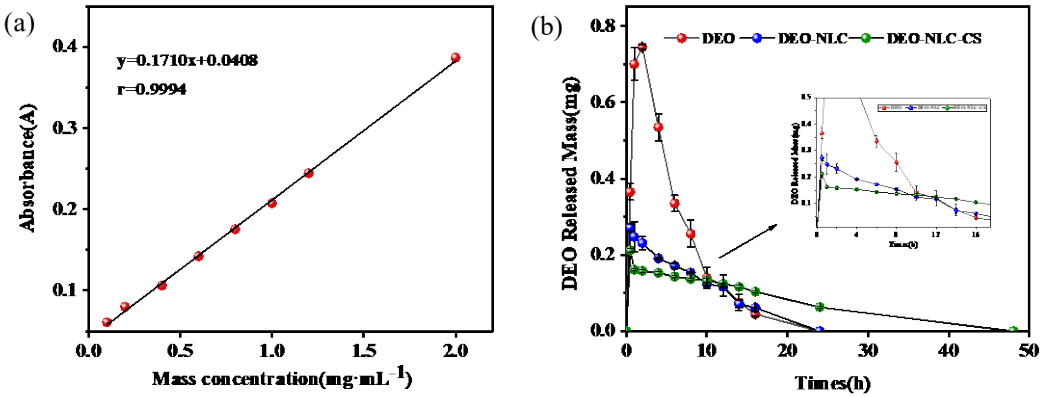

Fig. 5. (a) Standard curve of release medium (PBS solution); **(b)***In vitro* release profiles.

Storage stability study

The storage stability of DEO-NLC and DEO-NLC-CS was investigated at 25 °C without light and ventilation. From Fig. 6**(a)** and 6**(b)**, it can be seen that the average diameter of DEO-NLC and DEO-NLC-CS changed almost nothing after one month. However, the Zeta potential of DEO-NLC gradually increased, while the potential of DEO-NLC-CS did not change significantly (Fig. 6**(c)**). On the 15th day, DEO-NLC appeared flocs, while DEO-NLC-CS had no change (Fig. 6**(d)**).

PDI can reflect the width of particle diameter distribution. The smaller value can get a more uniform particle diameter and a more concentrated distribution of particle diameter [42]. Both particles showed a significant decrease in PDI in the third week (Fig. 6**(a)**, 6**(b)**). This may be due to the accelerated movement

J. Mex. Chem. Soc. **2026**, *70(1):e2165*
Regular Issue

ISSN-e 2594-0317

between particles caused by weather changes, and the dispersion improves [51]. The results above showed that the stability of DEO-NLC-CS was stronger than that of DEO-NLC.

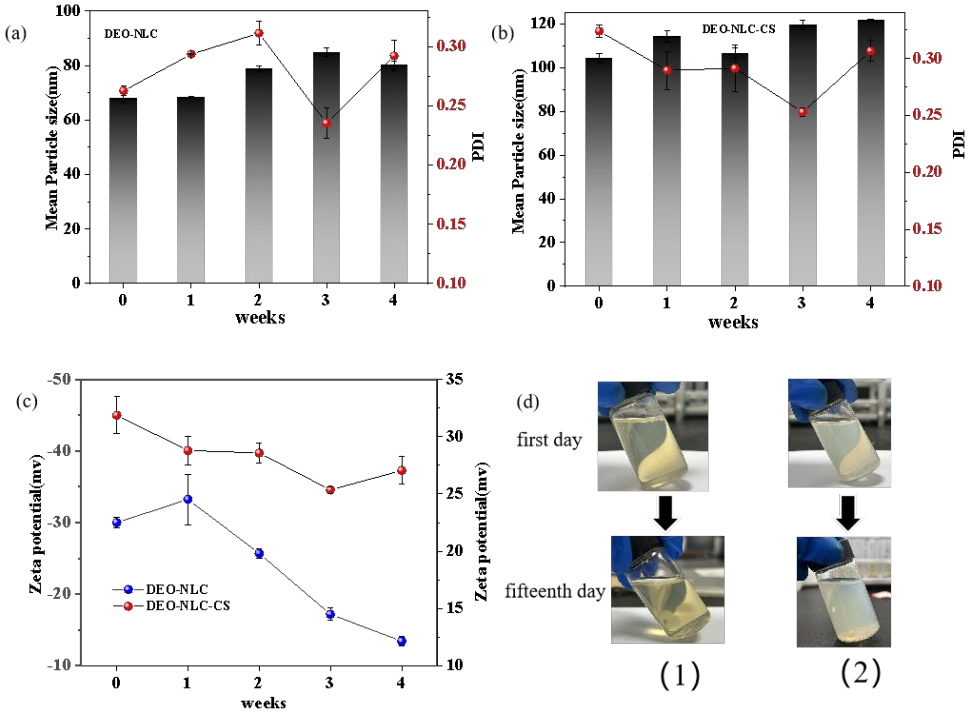

Fig. 6. (a) The diameter distribution of DEO-NLC after storage for 1 month; **(b)** The diameter distribution of DEO-NLC-CS after storage for 1 month; **(c)** The variation in Zeta potential during storage for 1 month; **(d)** Phenomena of the particles on the first day and the fifteenth day. Values were presented as mean ± SD (n=3).

Antioxidant activity

The DPPH free radical scavenging experiments of pure NLC, DEO-NLC, and DEO-NLC-CS showed that the encapsulated particles still had good antioxidant activity. Their ability to scavenge DPPH free radicals was concentration-dependent. The DPPH free radical scavenging ability increased with the increase of concentration (Fig. 7). Among them, blank NLC still had high free radical scavenging activity, which is attributed to the soybean lecithin (the main component of NLC), soybean lecithin has good antioxidant properties [52].

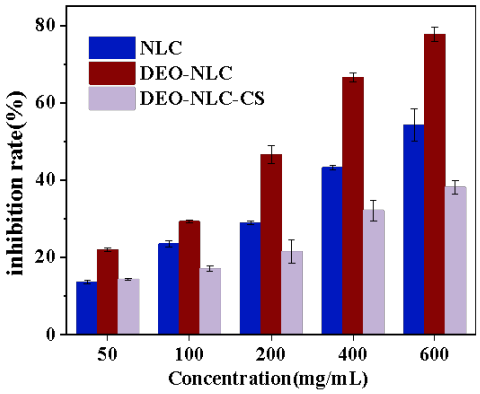

Fig. 7. DPPH radical inhibition of NLC, DEO-NLC, and DEO-NLC-CS at various concentrations.

http://dx.doi.org/10.29356/jmcs.v70i1.2165

J. Mex. Chem. Soc. **2026**, *70(1):e2165*
Regular Issue

ISSN-e 2594-0317

Conclusions

In this study, the *D. asper* essential oil (DEO) was successfully extracted by a supercritical CO_2 extraction device, and the NLC loaded with DEO was synthesized by melt emulsification-ultrasonic dispersion method, which solved the problem of easy-volatilization and instability. The prepared DEO-NLC was coated with chitosan to overcome the shortcomings of easy aggregation and poor dispersion of DEO-NLC at room temperature for a long time. Since the prepared DEO was found to have good oxidation resistance in the previous experiments, DEO-NLC and DEO-NLC-CS were used for the preliminary investigation of oxidation resistance. The results showed that the above two nanoparticles still preserved the good oxidation resistance of DEO. Both DEO-NLC and DEO-NLC-CS had the characteristics of small average diameter, uniform distribution, high encapsulation efficiency drug loading, and good sustained release performance. ATR-FTIR, DSC, and XRD studies showed the DEO was successfully encapsulated in the above two nanoparticles. This work overcomes important challenges, such as the instability of DEO.

Acknowledgements

Th is work is supported by the Sichuan Science and Technology Program (2022YFS0443) and the Science and Technology Research Project of the Sichuan Provincial Administration of Traditional Chinese Medicine (2023MS334).

References

1. Landis, R. F.; Gupta, A.; Lee, Y. W.; Wang, L. S.; Golba, B.; Couillaud, B.; Ridolfo, R.; Das, R.; Rotello, V. M. *ACS. Nano.* **2017**, *11*, 1, 946-952. DOI: https://doi.org/10.1021/acsnano.6b07537
2. Negi, A.; Kesari, K. K. *Micromachines.* **2022**, *13*, 8, 1265. DOI: https://doi.org/10.3390/mi13081265
3. Saporito, F.; Sandri, G.; Bonferoni, M. C.; Rossi, S.; Boselli, C.; Icaro Cornaglia, A.; Mannucci, B.; Grisoli, P.; Vigani, B.; Ferrari, F. *Int. J. nanomedicine.* **2018**, *13*, 8, 175-186. DOI: https://doi.org/10.2147/IJN.S152529
4. Trifan, A.; Luca, S. V.; Greige-Gerges, H.; Miron, A.; Gille, E.; Aprotosoaie, A. C. *Crit. Rev. Microbiol*. **2020**, *46*, 3, 338-357. DOI: https://doi.org/10.1080/1040841X.2020.1782339
5. Wu, Q.; Yang, Z.; Nie, Y.; Shi, Y.; Fan, D. *Cancer. lett.* **2014**, *347*, 2, 159-166. DOI: https://doi.org/10.1016/j.canlet.2014.03.013
6. Seibert, J. B.; Viegas, J. S. R.; Almeida, T. C.; Amparo, T. R.; Rodrigues, I. V.; Lanza, J. S.; Frézard, F. J. G.; Soares, R.; Teixeira, L. F. M.; de Souza, G. H. B.; Vieira, P. M. A.; Barichello, J. M.; Dos Santos, O. D. H. *J. Nat. Prod*. **2019**, *82*, 12, 3208-3220. DOI: https://doi.org/10.1021/acs.jnatprod.8b00870
7. Wu, H.; Moser, C.; Wang, H. Z.; Høiby, N.; Song, Z. *J. Int. J. Oral. Sci.* **2015**, *7*, 1, 1-7. DOI: https://doi.org/10.1038/ijos.2014.65
8. Diniz do Nascimento, L.; Moraes, A. A. B.; Costa, K. S. D.; Pereira Galúcio, J. M.; Taube, P. S.; Costa, C. M. L.; Neves Cruz, J.; de Aguiar Andrade, E. H.; Faria, L. J. *G. Biomolecules.* **2020**, *10*, 7, 988. DOI: https://doi.org/10.3390/biom10070988
9. Soltanzadeh, M.; Peighambardoust, S. H.; Ghanbarzadeh, B.; Mohammadi, M.; Lorenzo, J. M. *Int. J. Biol. Macromol.* **2021**, *192*, 1084-1097. DOI: https://doi.org/10.1016/j.ijbiomac.2021.10.070
10. Dong, N. N.; Chen, X. L.; Deng, B. L.; Xie, S. C.; Hu, J. *J. Chin. Mater. Med.* **2023**, *48*, 4,1076-1086. DOI: https://10.19540/j.cnki.cjcmm.20221102.703
11. Moreira, P.; Matos, P.; Figueirinha, A.; Salgueiro, L.; Batista, M. T.; Branco, P. C.; Cruz, M.T.; Pereira, C. F. *Int. J. Mol. Sci.* **2022**, *23,* 15, 8812. DOI: https://doi.org/10.3390/ijms23158812

J. Mex. Chem. Soc. **2026**, *70(1):e2165*
Regular Issue

ISSN-e 2594-0317

12. Qin, T. T.; Xie, H. X.; Hu, J. W.; Zeng, J. S.; Liu, R.; Zeng, N. *J. Chin. Mater. Med.* **2023**, *48*, 4, 1066-1075. DOI: https://10.19540/j.cnki.cjcmm.20221014.705
13. Silva, P.; Rodríguez-Pérez, M.; Gómez-Torres, Ó.; Burgos-Ramos, E. *Nutr. Res. Rev.* **2023**, *36,* 1, 140-154. DOI: https://doi.org/10.1017/S095442242100041X
14. Luo, J. F.; Zhou, H.; Lio, C. K. *Molecules(Basel,Switzerland).* **2022**, *27,* 19, 6236. DOI: https://doi.org/10.3390/molecules27196236
15. Xi, Y.; Zhao, T.; Shi, M.; Zhang, X.; Bao, Y.; Gao, J.; Shen, J.; Wang, H.; Xie, Z.; Wang, Q.; Li, Z.; Qin, D. *Evid. Based. Complement. Alternat. Med.* **2023,** *2023*, 2140327. DOI: https://doi.org/10.1155/2023/2140327
16. Yao, W. L.; Pan, J.; Niu, T. F.; Yang, X. L.; Zhao, S. J.; Wang, Z. T.; Wang, R. F. *Chin. Mater. Med.* **2022**, *47*, 17, 4593-4599. DOI: https://10.7501/j.issn.0253-2670.2013.11.022
17. Tian, S.; Zou, Y.; Wang, J.; Li, Y.; An, B. Z.; Liu, Y. Q. *J. Ethnopharmacol.* **2022**, *295*, 115399. DOI: https://doi.org/10.1016/j.jep.2022.115399
18. Karimi, N.; Ghanbarzadeh, B.; Hamishehkar, H.; Mehramuz, B.; Kafil, H. S. *Colloids. Interface. Sci. Commun.* **2018**, *22*, 18-24. DOI: https://doi.org/10.1016/j.colcom.2017.11.006
19. Liu, B.; Kou, J.; Li, F.; Huo, D.; Xu, J.; Zhou, X.; Meng, D.; Ghulam, M.; Artyom, B.; Gao, X.; Ma, N.; Han, D. *Aging.* **2020**, *12,* 9, 8622-8639. DOI: https://doi.org/10.18632/aging.103179
20. Cai, M.; Wang, Y.; Wang, R.; Li, M.; Zhang, W.; Yu, J.; Hua, R. *Int. J. Biol. Macromol.* **2022**, *202*, 122-129. DOI: https://doi.org/10.1016/j.ijbiomac.2022.01.066
21. Miranda, M.; Cruz, M.T.; Vitorino, C.; Cabral, C. *Mater. Sci. Eng. C. Mater. Biol. Appl.* **2019**, *103*, 109804. DOI: https://doi.org/10.1016/j.msec.2019.109804
22. Tenchov, R.; Bird, R.; Curtz, A. E.; Zhou, Q. *ACS. Nano.* **2021**, *15*, 11, 16982-17015. DOI: https://doi.org/10.1021/acsnano.1c04996
23. Wu, B.; Li, Y.; Li, Y. Y.; Shi, Z. H.; Bian, X. H.; Xia, Q. *J. Biomater. Appl.* **2022,** *36*, 8, 1444-1457. DOI: https://doi.org/10.1177/08853282211053923
24. Bashiri, S.; Ghanbarzadeh, B.; Ayaseh, A.; Dehghannya, J.; Ehsani, A. *LWT.* **2020**, *119*, 108836. DOI: https://doi.org/10.1016/j.lwt.2019.108836
25. Yostawonkul, J.; Surassmo, S.; Iempridee, T.; Pimtong, W.; Suktham, K.; Sajomsang, W.; Gonil, P.; Ruktanonchai, U. R. *Colloids. Surf. B.* **2017**, *149*, 301-311. DOI: https://doi.org/10.1016/j.colsurfb.2016.09.049
26. Wang, M.; Zhao, T.; Liu, Y.; Wang, Q.; Xing, S.; Li, L.; Wang, L.; Liu, L.; Gao, D. *Mater. Sci. Eng. C. Mater. Biol. Appl.* **2017**, *71*, 1231-1240. DOI: https://doi.org/10.1016/j.msec.2016.11.014
27. Hasan, M.; Elkhoury, K.; Belhaj, N.; Kahn, C.; Tamayol, A.; Barberi-Heyob, M.; Arab-Tehrany, E.; Linder, M. *Mar. Drugs.* **2020**, *18*, 4, 217. DOI: https://doi.org/10.3390/md18040217
28. Ramezanzade, L.; Hosseini, S. F.; Nikkhah, M. *Food. Chem.* **2017**, *234*, 220-229. DOI: https://doi.org/10.1016/j.foodchem.2017.04.177
29. Tan, C.; Zhang, Y.; Abbas, S.; Feng, B.; Zhang, X.; Xia, S.; Chang, D. *Food. Funct.* **2015**, *6*,12, 3702-3711. DOI: https://doi.org/10.1039/c5fo00256g
30. Du, W.; Li, X.; Yang, Y.; Yue, X.; Jiang, D.; Ge, W.; Cai, B. *Pharm. Biol.* **2017**, *55*, 1, 2129-2135. DOI: https://doi.org/10.1080/13880209.2017.1297469
31. Molino, A.; Mehariya, S.; Iovine, A.; Larocca, V.; Di Sanzo, G.; Martino, M.; Casella, P.; Chianese, S.; Musmarra, D. *Mar. Drugs.* **2018**, *16,* 11, 432. DOI: https://doi.org/10.3390/md16110432
32. Ruan, N.; Jiao, Z.; Tang, L. J. *AOAC. Int*. **2022**, *105*, 1, 272-281. DOI: https://doi.org/10.1093/jaoacint/qsab108.
33. Soh, S. H.; Lee, L. Y. *Pharmaceutics.* **2019**, *11,* 1, 21. DOI: https://doi.org/10.3390/pharmaceutics11010021
34. Kuś, P. M.; Okińczyc, P.; Jakovljević, M.; Jokić, S.; Jerković, I. *J. Pharm. Biomed. Anal.* **2018**, *158*, 15-27. DOI: https://doi.org/10.1016/j.jpba.2018.05.041
35. Wang, J.; Wang, H.; Xu, H.; Li, J.; Zhang, X.; Zhang, X. *RSC. Adv.* **2022**,*12*,11,6583-6591. DOI: https://doi.org/10.1039/d1ra07638h

J. Mex. Chem. Soc. **2026**, *70(1):e2165*
Regular Issue

ISSN-e 2594-0317

36. Yao, K.; Ma, Y. Z.; Yi, G. H.; Wang, Y. X.; Zhou, X.; Zang, X.; Liu, Y. Q.; Wang, T.; He, X.W. *Chin. J. Trop. Crops.* **2022**, 44, 7, 1478-1487. DOI: https://doi.org/10.3969/j.issn.1000-2561.2023.07.019
37. Lee, S. A.; Joung, H. J.; Park, H. J.; Shin, G. H. *J. Food. Sci.* **2017**, *82,* 4, 904-912. DOI: https://doi.org/10.1111/1750-3841.13655
38. Kumbhar, D. D.; Pokharkar, V. B. *Colloid. Surface. A.* **2013**, *416*, 32-42. DOI: https://doi.org/10.1016/j.colsurfa.2012.10.031
39. outo, E. B.; Müller, R. H. *J. Microencapsul.* **2005**, *22*, 501-510. DOI: https://doi.org/10.1080/02652040500162436
40. Keivani Nahr, F.; Ghanbarzadeh, B.; Hamishehkar, H.; Samadi Kafil, H. *J. Funct. Foods.* **2018**, *40*, 1-8. DOI: https://doi.org/10.1016/j.jff.2017.09.028
41. Hu, Q.; Zhou, F.; Ly, N. K.; Ordyna, J.; Peterson, T.; Fan, Z.; Wang, S. *ACS. Nano.* **2023**, *17*, 8586-8597. DOI: https://doi.org/10.1021/acsnano.3c01094
42. Teeranachaideekul, V.; Boonme, P.; Souto, E. B.; Müller, R. H.; Junyaprasert, V. B. *J. Control. Release.* **2008**, *128*, 134-141. DOI: https://doi.org/10.1016/j.jconrel.2008.02.011
43. Chaiyasan, W.; Srinivas, S. P.; Tiyaboonchai, W. *Mol. Vis.* **2015**, *21*, 1224-1134. DOI: https://10.1016/J.IJPHARM.2021.121287
44. Sun, R.; Xia, Q. *Colloid. Surface. A.* **2019**, *574*, 197-206. DOI: https://doi.org/10.1016/j.colsurfa.2019.04.082
45. Pardeike, J.; Hommoss, A.; Müller, R. H. *Int. J. Pharm.* **2009**, *366,* 170-184. DOI: https://doi.org/10.1016/j.ijpharm.2008.10.003
46. Rai, N.; Madni, A.; Faisal, A.; Jamshaid, T.; Khan, M. I.; Khan, M. M.; Parveen, F. Curr. Drug. Deliv. **2021**, *18*, 1368-1376. DOI: https://doi.org/10.2174/1567201818666210203180153
47. Yui, T.; Uto, T.; Ogawa, K. *Nanomaterials (Basel, Switzerland).* **2021**, *11*, 6, 1407. DOI: https://doi.org/10.3390/nano11061407.
48. Averina, E. S.; Seewald, G.; Müller, R. H.; Radnaeva, L. D.; Popov, D. V. *Pharmazie.* **2010**, *65*, 1, 25-31. DOI: https://10.1691/ph.2010.9203
49. Mendes, A. I.; Silva, A. C.; Catita, J. A.; Cerqueira, F.; Gabriel, C.; Lopes, C. *Colloids. Surf. B.* **2013**, *111*, 755-763. DOI: https://doi.org/10.1016/j.colsurfb.2013.05.041
50. Hu, Q.; Lu, Y.; Luo, Y. *Carbohydr. Polym.* **2021**, *264*, 117999. DOI: https://doi.org/10.1016/j.carbpol.2021.117999
51. Araújo, J.; Nikolic, S.; Egea, M.A.; Souto E.B.; Garcia M.L. *Colloids and Surfaces B: Biointerfaces*, **2011**, *88*, 150–157. DOI: https://doi.org/10.1016/j.colsurfb.2011.06.025
52. Yang, Y.H.; Pan, H.Z.; Song, B.J.; Zhu, X.J.; Sun, Y.W. *Prog. Modern. Biomed.* **2011**, *11*, 4024-4026. DOI: 10.13241/j.cnki.pmb.2011.21.006